

A Theory of the Pattern Induced Flight Orientation of the Fly *Musca Domestica* II

Werner Reichardt and Tomaso Poggio

Max-Planck-Institut für biologische Kybernetik, Tübingen, FRG

Received: July 10, 1974

Abstract

In a preceding paper, Poggio and Reichardt (1973a), a phenomenological theory describing the visual orientation behaviour of fixed flying flies (*Musca domestica*) towards elementary patterns was presented. Some of the problems raised in this first paper are treated here in more detail. The mapping between the position dependent torque distribution — $D(\psi)$ characteristics — associated with a given pattern and the stationary orientation distribution $p(\psi)$, is studied taking into account that the fluctuation process (generated by the fly) is coloured gaussian noise. Under certain critical conditions this may lead to an "early symmetry breaking" in the mean values of the $p(\psi)$ distribution. The validity of the "superposition principle" has also been examined. Although shift and superposition give the main qualitative features of the "attractiveness profile" $D(\psi)$, associated with a 2-stripe pattern, superposition does not hold quantitatively for stripe separations up to about 80° . Evidence is presented suggesting that such an effect is due to inhibitory interactions between input channels of the fly's eye. Implications of this finding with respect to the problem of spontaneous pattern preference are also discussed.

Introduction

In the two preceding papers, Reichardt (1973), Poggio and Reichardt (1973a), we have investigated the visual orientation behaviour of fixed flying flies (*Musca domestica*) under the condition of one dynamic degree of freedom: the rotation of the fly around its vertical axis. In the first paper a sequence of experimental results was presented which in turn led to a theoretical treatment, published in the second paper. The theory is entirely based on quantitative behavioural results and therefore is a phenomenological description whose logical role can be compared with a thermodynamic approach in physics. In order to bridge the gap between the phenomenological level and the underlying nervous mechanisms, a conceptual framework dealing with the functional properties of these mechanisms was developed in a third paper, Poggio and Reichardt (1973b). This framework is the next

logical step in the analysis since it takes into consideration the interaction processes between the signals from individual light receptors.

The purpose of the present investigation is to examine in more detail some of the problems outlined in the second paper, Poggio and Reichardt (1973a), from both the experimental and the theoretical points of view — always at the phenomenological level. There are essentially two problems:

a) The phenomenological equations, linking the pattern induced flight torque response with the fly's orientation behaviour, have so far only been applied to those orientation tasks which allow a linearization of the equations. However, in our theoretical considerations we also took into account the nonlinear part of the problem, under the simplifying assumption that the torque fluctuation $N(t)$, generated by the fly, can be approximated by gaussian white noise. A quantitative comparison between experiments and theoretical predictions, using the actual properties of $N(t)$, is made in this paper. As mentioned in the first paper, our theory can also be applied to tracking situations. Experimental evidence in agreement with the theoretical predictions is presented here for a simple tracking task.

b) Earlier experiments, Reichardt (1973), have suggested that the orientation behaviour of the fly towards a panorama, consisting of a collection of elementary objects, such as vertically oriented stripes or stripe segments, can be derived from the superposition of the responses elicited by each object independently. These suggestions are examined in more detail in this paper and lead to some new insights into the functional properties of the underlying mechanisms.

The conceptions and the experimental methods are the same as described before, Reichardt (1973) and Poggio and Reichardt (1973a).

The Mapping of the Potential-Distributions into the Flight-Orientation Distributions

Before turning to the experiments, we would like to recall the phenomenological description of the orientation behaviour, originally outlined in Poggio and Reichardt (1973 a). The equation for the rotatory degree of freedom $\psi(t)$ reads

$$\Theta \ddot{\psi}(t) + k\dot{\psi}(t) = N(t) - F\{\psi(t), \dot{\psi}(t)\}. \quad (1)$$

The left side of Eq. (1) represents an approximation to the dynamics of free flight, whereas the right side consists of two terms: the torque fluctuation $N(t)$ and the optomotor response F , defined as the "open loop" response to moving stimuli. Since the fly's reaction under normal fixation mainly depends on the instantaneous values of ψ and $\dot{\psi}$, the functional $F\{\psi(t), \dot{\psi}(t)\}$ reduces to a function of ψ and $\dot{\psi}$ which can be written as

$$F[\psi(t), \dot{\psi}(t)] = D^\dagger[\psi(t), \dot{\psi}(t)] + \varrho[\psi(t), \dot{\psi}(t)], \quad (2)$$

where D^\dagger represents its even part and ϱ its odd part in $\dot{\psi}$. It has been shown experimentally under normal conditions of coupling between the test-fly and the panorama that Eq. (2) can be approximated by a linear expression in $\dot{\psi}$ which reads:

$$F = -D[\psi(t)] + r\dot{\psi}(t) \quad (3A)$$

or

$$F = + \frac{\partial}{\partial \psi} U[\psi(t)] + r\dot{\psi}(t), \quad (3B)$$

where U is the "potential" associated with D .

It should be pointed out that our description of F is based on a "quasistationary" phenomenological approximation neglecting the dynamics of the fly's reaction. This simplification is the basic reason why Eq. (3A) is only valid for $\overline{\dot{\psi}^2} > 0$ (see Appendix I). In order to examine experimentally the mapping of potential-distributions into flight orientation-distributions, the corresponding potentials of panoramas, containing one or two black, vertically oriented stripes, have been measured under strictly open-loop conditions. Previously, Reichardt (1973), Poggio and Reichardt (1973 a), the experimental determination of $D(\psi)$ and $U(\psi)$ has been carried out under partial closed-loop conditions. That is, the panorama was coupled to the test-fly but in addition elastically bound to a position $\psi = \psi_0$. During the experiments presented here, the test-fly was not coupled to the panorama (open-loop conditions). The panorama was symmetrically moved with randomly distributed speeds and maximum amplitudes of about ± 5 degrees around a given angular position ψ_0 . The power spectrum of the random signal was tuned to the fly's noise torque

spectrum, measured under closed-loop condition. Comparing the results obtained under partial closed and open-loop conditions, we have observed that they are in basic agreement with one another. However, in the open-loop technique the reactions measured are strictly related to the selected ψ -position whereas in the partially closed-loop case the selected (average) ψ -position is systematically shifted (maximally about 5–10 degrees) towards the direction of flight.

The averages from measurements of $D(\psi)$ and the corresponding $U(\psi)$ for the different one and two stripe patterns are presented in Fig. 1 a and b respectively. Parameter of the experiments is the separation angle $\Delta\psi$ (center to center) between the two stripes. If one inspects the $D(\psi)$ and corresponding $U(\psi)$ distributions one recognizes a flattening in the potential minimum with increasing $\Delta\psi$ which finally result in a build up of two minima.

In order to work out the mapping of the $D(\psi)$ or $U(\psi)$ distributions presented in Fig. 1, into the associated stationary position-probability $p(\psi)$, $D(\psi)$ has to be introduced into the phenomenological Eqs. (1) and (3). In one of the preceding papers, Poggio and Reichardt (1973 a), an analytical solution of the equation was given under the assumption that $N(t)$ is a gaussian white noise process. In fact the fly generates a gaussian torque fluctuation $N(t)$ whose spectral composition is not white. Under these conditions only an approximate solution can be given, see Appendix II. Therefore the stationary probability distribution $p(\psi)$ was obtained through a digital simulation of Eqs. (1) and (3). The simulations were carried out with a coupling value of $\frac{\Theta}{k} = 8 \cdot 10^{-3}$ sec, and numerical values of $N(t)$ and r which had been specified before, Poggio and Reichardt (1973 a). One should however be aware of the fact that the numerical values of these parameters vary to some extent from fly to fly. The $p(\psi)$ distributions, obtained from the computer simulations, are presented together with the ones actually measured in Fig. 2 a and b respectively. Comparing the computer simulated $p(\psi)$ distributions with the experimental ones, one observes somewhat sharper fixations in the simulations. Deviations between the two sets are especially pronounced in the critical phase transition range ($\Delta\psi$ between 40° and 60°) where the one-maximum in the $p(\psi)$ -distribution breaks into a two-maxima configuration. These observations have two causes: as we have stated before, the power of the torque noise $N(t)$, generated by the flies, shows some variability from fly to fly. In our simulations we have applied an $N(t)$ -power which has been specified before, Poggio and Reichardt (1973 a), and seems rather typical for the

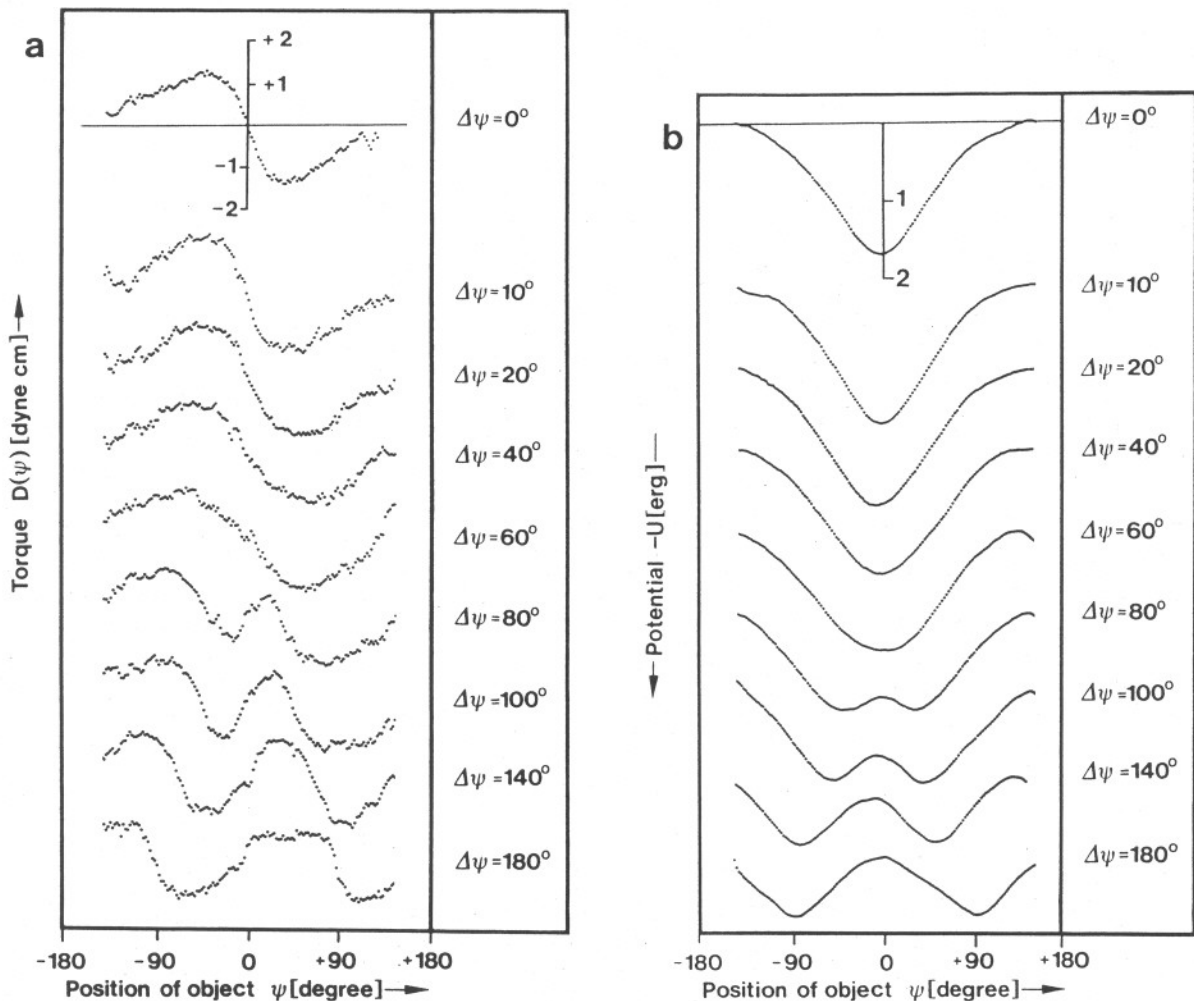


Fig. 1. (a) The "attractiveness" profiles $D(\psi)$ of 1- and 2-stripe patterns: parameter is the angular separation $\Delta\psi$ between the stripes (5° wide). The pattern was symmetrically moved with a maximum amplitude of $\pm 5^\circ$ around each angular position ψ : the torque generated by the fly was recorded under open-loop conditions. The distributions presented in the figure are each averages of 6–15 individuals, and agree well with equivalent measurements performed under partially closed-loop conditions. (b) "Potentials" $U(\psi)$ formally derived from the $D(\psi)$

distributions of Fig. 1a according to the relation $-\frac{\partial U(\psi)}{\partial \psi} = D(\psi)$

test-flies. The second cause is the technique applied in the experiments in order to determine the shape of the $D(\psi)$ distributions. That is, the test-panoramas were moved stochastically around a given ψ -position by about $\pm 5^\circ$. This procedure of course introduces some smoothing of the shapes of the $D(\psi)$ distributions which in turn especially affects the critical range of these $\Delta\psi$ where the two minima in the potential distributions build up. In Fig. 3 we have plotted the separation angle $\Delta\psi_{\text{exp}}^*$ versus the separation angle $\Delta\psi_{\text{simul.}}^*$ for the $p(\psi)$ distributions with two maxima. The plot shows that there is very good agreement in the range $80^\circ < \Delta\psi < 180^\circ$, whereas the point at $\Delta\psi = 60^\circ$ does significantly deviate from the 45° line,

$\Delta\psi_{\text{exp.}}^*$ having a greater value than $\Delta\psi_{\text{simul.}}^*$. This observation varies from fly to fly and eventually the two $\Delta\psi^*$ -values are equal even in this critical region. The disagreement between the two $\Delta\psi^*$ -values, mostly found near or in the critical region of the symmetry breaking in the potential-distribution, could be accounted for by the smoothing of the $D(\psi)$ -distributions, which, as has been discussed before, is a consequence of the experimental method.

The effect discussed here is enhanced by the influence of the non-white spectral composition of the noise $N(t)$. As it is shown in Appendix II the non-white noise character of the fluctuation $N(t)$ can produce a two-maxima fixation-distribution even if

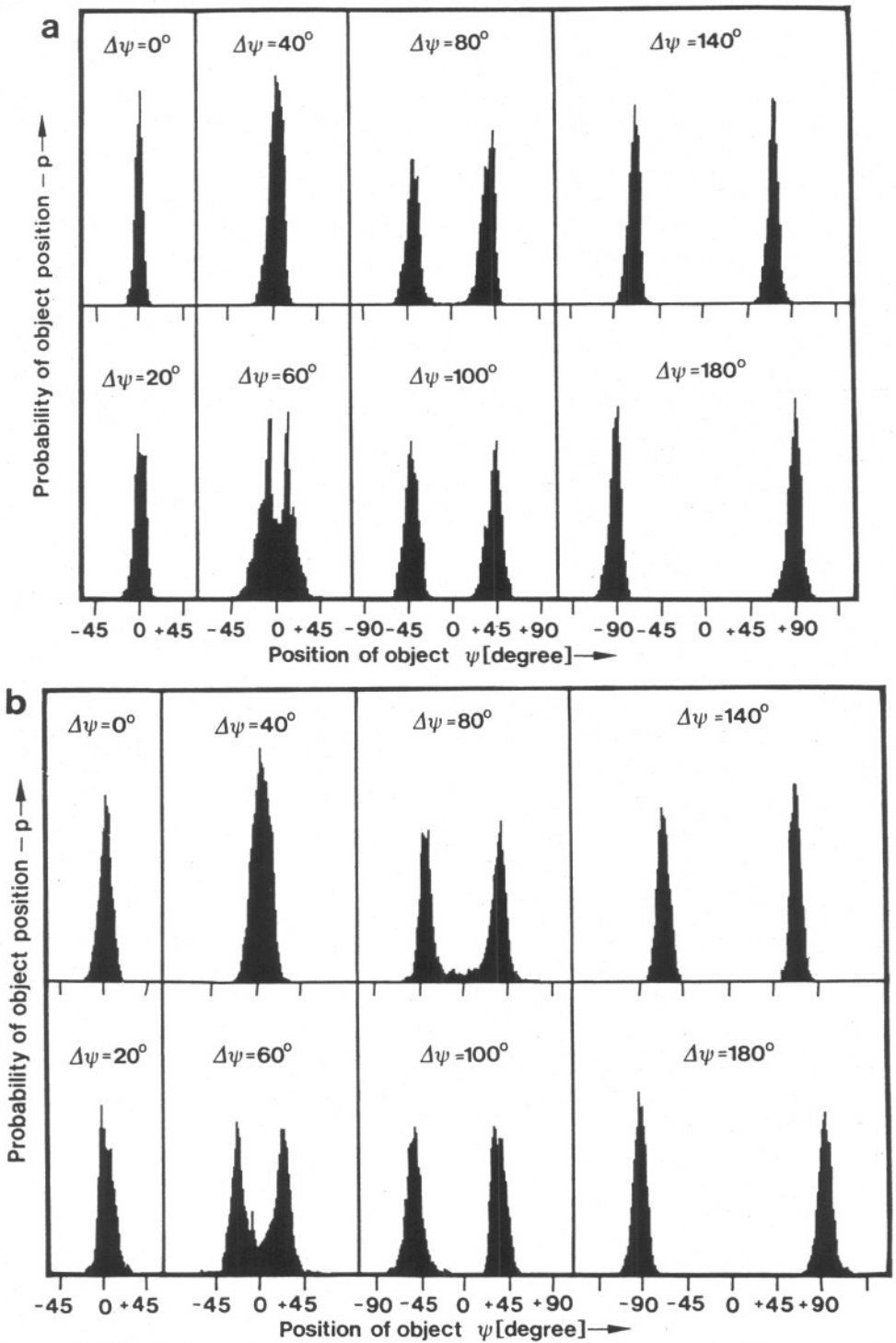


Fig. 2. (a) Stationary probability distributions $p(\psi)$, obtained from digital simulation of the Eqs. (1) and (3A). The $D(\psi)$ characteristics in Fig. 1a have been used in the simulations; the values of the other parameters are the ones used in Poggio and Reichardt. The numerical values of the parameters are $\frac{\Theta}{k} = 8 \cdot 10^{-3}$ sec, $\frac{r}{\Theta} = 60 \text{ sec}^{-1}$, $\sqrt{A} = 0.3$ dyn cm, $\gamma = 1.9 \text{ sec}^{-1}$. The equivalent duration of the simulated experiments was either 3 min (for $\Delta\psi = 0^\circ$ and $\Delta\psi = 20^\circ$) or 2×3 min. The normalization of the histograms is only approximately similar to the one used in Fig. 2b. (b) Position histograms, obtained from single test flies during the stationary fixation of 1-patterns. Parameter is $\Delta\psi$ as before. The coupling constant amounts to $\frac{\Theta}{k} = 8 \cdot 10^{-3}$ sec. The duration of the experiments is the same as in Fig. 2a.

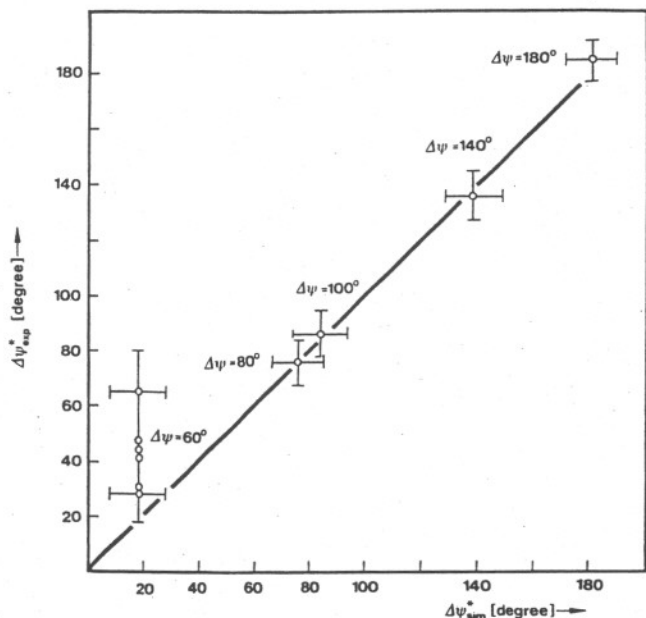


Fig. 3. The angular separation $\Delta\psi_{exp}^*$ for the experimental two maxima distributions (evaluated from their cumulative probability density) is plotted here against the angular separation $\Delta\psi_{sim}^*$ pertaining to the simulations. The data are read from Fig. 2a and b; for the point $\Delta\psi = 60^\circ$, data from other individuals are also shown. No such scatter was observed for the other points

the associated potential-distribution still has one minimum; an effect which may be called an "early phase transition". The size of the effect strongly depends on the shape of the potential: for instance a kink in the potential favours an early phase transition with respect to the maxima of the histogram.

Equations (1) and (3A) can easily be extended to describe the average fly's behaviour under visual tracking tasks. For instance if an object moves with constant speed, the fly will track it (and lose it from time to time, depending on the speed value) with a phase lag, Virsik and Reichardt (1974). Under quasi-stationary conditions (speed not too high), Eq. (III-1) can be used directly to provide the steady-state probability distribution of ψ . Under the assumption of $N(t)$ being white gaussian noise, an analytical solution can be given (see Appendix III). In Fig. 4 an experimentally obtained probability distribution is compared with another one generated by a digital simulation of the dynamic equation (with the actual coloured noise spectrum). Similar experiments with two stripe patterns have also shown a satisfactory agreement with the theoretical predictions. In summary: the phenomenological equation describing the mapping of the open-loop reaction into the closed-loop orienta-

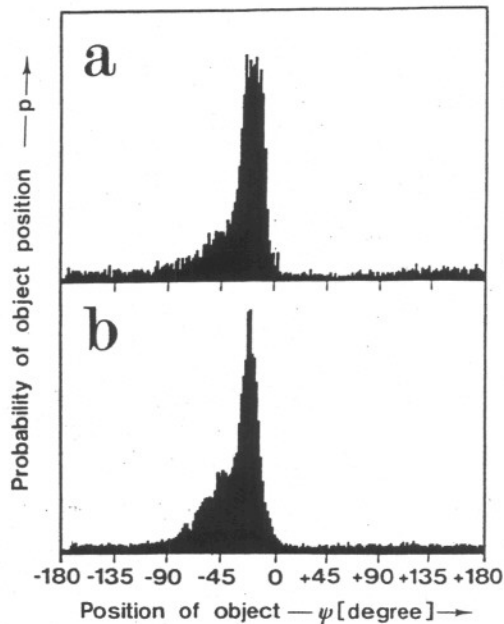


Fig. 4a and b. Theoretical (a) and experimental (b) histograms of the stripe position in a tracking experiment in which a constant voltage was added to the servomotor system simulating a stripe moving at constant angular speed. The experimental histogram (b) is typical for a test fly but a large amount of individual variability is observed; the histogram (a) has been obtained through a digital simulation of the equation (see also Appendix III) $\Theta\dot{\psi} + (k+r)\psi + D(\psi) = N(t) + V$, where the parameter values are the same as indicated in Fig. 2a and $D(\psi)$ is the first distribution (for the 1-stripe pattern) of Fig. 1a. V was chosen such that the same rate of target loss was observed during the experiments. The fact that the peak of the distributions is shifted with respect to $\psi = 0^\circ$ means that the fly tracks the stripe, moving at constant speed, with a certain phase lag, which is quantitatively given by the phenomenological equation. Other experiments have extensively proved this theoretical prediction; Virsik and Reichardt (1974)

tion behaviour of the fly is in basic agreement with our observations, at least for simple orientation tasks as we have described here.

Additivity of Induced Torque Response: The Superposition Rule

In the preceding chapter we have presented a sequence of $D(\psi)$ and corresponding $U(\psi)$ distributions which were measured under open-loop conditions with panoramas consisting of one or two stripes. Fixation experiments with one, two and more stripes have been carried out earlier, see Reichardt (1973). Their results suggested that the stable orientation directions of a test-fly confronted with two or more stripes, are predictable from the $D(\psi)$ -characteristics of one stripe by shift and superposition. However, experiments testing the equilibrium positions can not

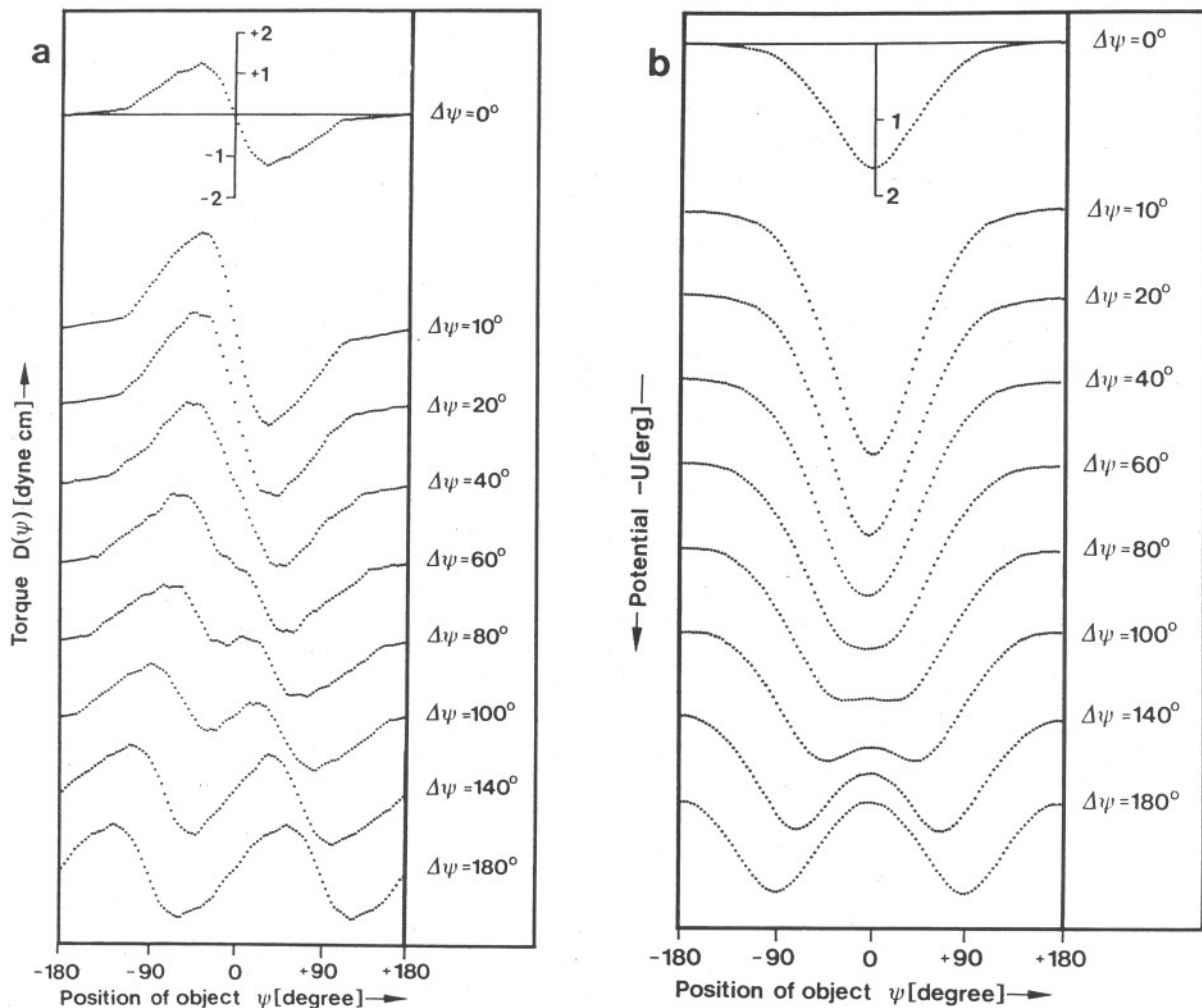


Fig. 5. (a) $D(\psi)$ distributions obtained by shift and superposition from the first distribution ($\Delta\psi = 0^\circ$), which represents a symmetrized copy of the experimentally measured $D(\psi)$ (Fig. 1a). The results represent the "attractiveness" profiles for the 2-stripe pattern provided that the "superposition rule" holds for all $\Delta\psi$ values. A comparison with Fig. 1 shows significant quantitative discrepancies. (b) Potential distributions associated to the $D(\psi)$ of Fig. 5a

reveal whether superposition of the individual $D(\psi)$ s holds in a strict sense or whether it has to be weighted by a (ψ -dependent) factor. In fact the superposition rule must fail when two or more stripes are brought into closest proximity since the corresponding $D(\psi)$ distributions can not reach very large values.

In order to investigate this problem in quantitative detail, we have constructed from a single stripe $D(\psi)$ -distribution by shift and superposition, a sequence of $D(\psi)$ - and $U(\psi)$ -distributions for the various two-stripe cases, characterized by the separation parameter $\Delta\psi$. These distributions are presented in Fig. 5a and b. A first comparison between the distributions in Fig. 5a and b and those actually measured in Fig. 2a and b shows that they are similar in shape; however, a closer inspection shows quantitative deviations. The location

of the minima in the potential distributions are important for the positions of the fixation maxima. In Fig. 6 we therefore compare the separation angles between the two minima in both cases. The plot in Fig. 6 shows that there is perfect agreement between the separation angles at 180° , 140° , and 100° . For the data presented in this paper, a deviation is found near the critical region at 80° . Here, the separation $\Delta\psi_{\text{exp}}^{**}$ between the minima in the potential distribution turns out to be larger than $\Delta\psi_{\text{sup}}^{**}$ in the case of superposition. Since the shapes of the $D(\psi)$ -distributions vary to some extent from fly to fly, the deviation at 80° may be due to the fact that different flies have been used in each set of experiments. These differences can lead to rather significant effects in the critical region of $\Delta\psi$ when two minima are emerging from one minimum

in the potential distributions. In fact, other data (for instance in Fig. 8) show that there can even be an agreement between the actually measured separation of minima and the one predicted from the single $D(\psi)$ -distribution. However, one can not exclude that the

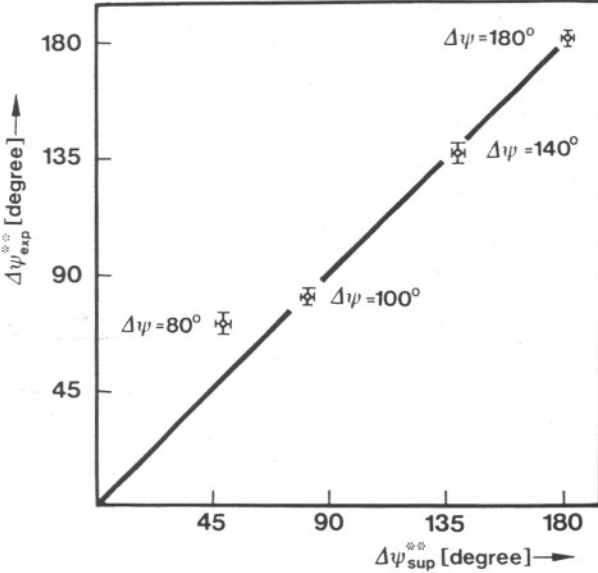


Fig. 6. The separation angles $\Delta\psi_{exp}^{**}$ between the minima of the experimentally measured potentials (Fig. 1b) are compared here with the separation angles $\Delta\psi_{sup}^{**}$ obtained through shift and superposition of the $D(\psi)$ profile, measured in the 1-stripe case. The deviation at $\Delta\psi = 80^\circ$ is probably not important, as Fig. 8 seems to suggest. However, with respect to the size of the minimum significant quantitative discrepancies are observed for lower values of $\Delta\psi$

deviation shown in Fig. 6 might depend on the inhibition which is discussed next.

As we have stated before, the quantitative details of the two-stripe $D(\psi)$ -distributions cannot be obtained through the superposition rule. The magnitudes of the $D(\psi)$ -distributions are reflected in the depths of the associated "potentials" which are presented in Fig. 7 as a function of the separation angle $\Delta\psi$ between the two stripes. The data plotted were taken from the actually measured distributions and those constructed by shift and superposition. The two curves in Fig. 7 are widely separated from one another in the region of small $\Delta\psi$. This mismatch diminishes with increasing $\Delta\psi$, but does not completely disappear even for large $\Delta\psi$. At first sight one is inclined to explain the differences between the two curves in Fig. 7 by assuming that the large values in the measured $D(\psi)$ distributions are bound by saturation of the reaction. This possibility is however ruled out by two observations: first, the slope of the linear part of the $D(\psi)$ distribution around $\psi = 0$ does not increase when the two stripes are displaced from zero to about 30° , as would be expected in the case of superposition, even in the presence of saturation. Second, equivalent experiments undertaken with short stripe segments, whose results are presented in Fig. 8, prove that a possible saturation can not be the main cause for the discrepancy between the two curves in Fig. 7. Therefore our conclusion is: the effects produced by the two stripes in the visual system of the fly are influenced by an inhibitory interaction which seems to be rather strong in the

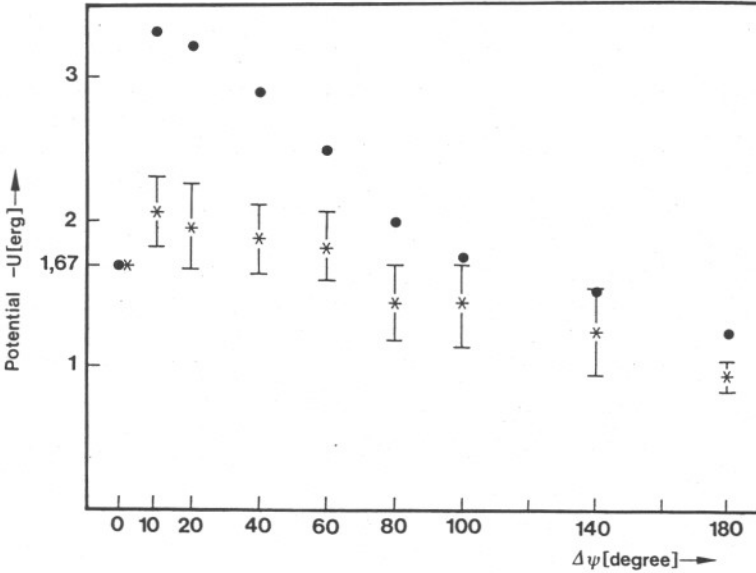


Fig. 7. Depth of the measured potentials of Fig. 1b (*) — in ergs — and of the potentials of Fig. 5b, obtained through the superposition rule (●)

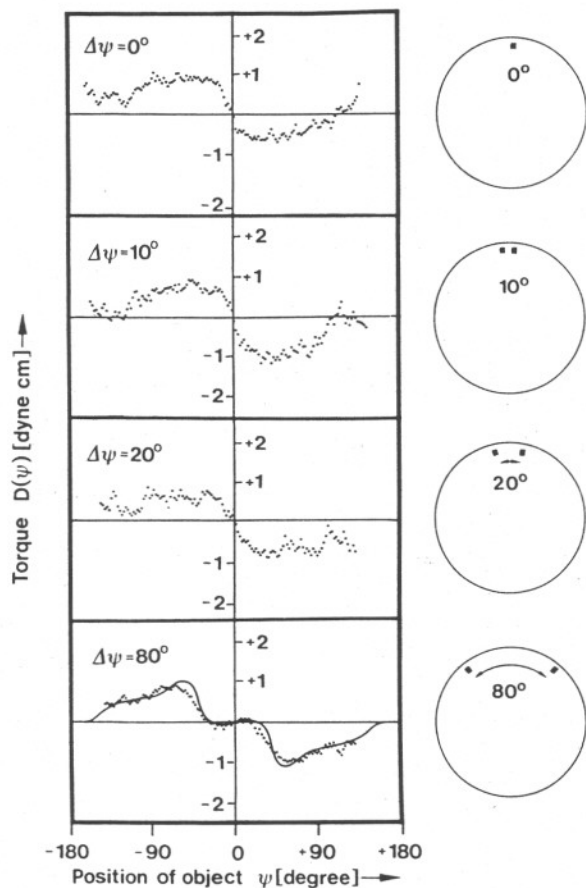


Fig. 8. In order to rule out a saturation effect as the possible cause for the quantitative failure of the superposition rule in the case of small $\Delta\psi$ values, $D(\psi)$ distributions have been measured for patterns consisting of smaller stripes. The individual stripe is 5° wide, has only $\frac{1}{4}$ length of the stripe normally used and it is located in the middle of the lower half of the cylinder. The torque generated by the fly is clearly smaller than in Fig. 1a; nevertheless shift and superposition of the distribution associated with $\Delta\psi = 0$ would not result in the distributions found for $\Delta\psi = 10^\circ$ and $\Delta\psi = 20^\circ$. However shift and superposition of the symmetrized 1-stripe $D(\psi)$ leads to a good approximation (continuous line) in the case $\Delta\psi = 80^\circ$. The distributions presented here are averages of 5 individual open-loop measurements

region $0^\circ < \Delta\psi < 60^\circ$. It is surprising that the weak mutual inhibition does not completely disappear in the region $60^\circ < \Delta\psi < 180^\circ$. We therefore believe that the significance of our observations in this region should still be considered as a somewhat open question.

In preceding papers, Poggio and Reichardt (1973a), Poggio (1974), a general description of the underlying nonlinear neural interactions has been discussed. It is important to realize in this context, that in the experiments presented in this chapter, the two objects

were moved coherently. In other experiments where the optomotor reaction to stripes of different widths was studied, it was observed that for stripe widths up to about $\Delta\psi \approx 40^\circ$ the total effect was less than the sum of the partial effects of the individual stripe edges, Geiger (1974), which is consistent with our observation. In these experiments the two edges moved coherently. Quite different are the results from experiments, Virsik and Reichardt (1974), where an object was moved incoherently with respect to a background consisting of visual noise. Under these conditions the observations suggest that – due to incoherence – the mutual inhibition between the effects released by the object and the background is destroyed as it may be in the case of nonlinear interactions. Experiments devised with the aim of characterizing the type of interactions in different parts of the compound eyes are now in progress in our laboratory.

Discussion

The interpretation of the experiments presented in this and in the preceding papers, Reichardt (1973), Poggio and Reichardt (1973a), is based on a phenomenological equation of motion in which the reaction of the fly to a moving pattern only depends on the instantaneous values of its position ψ and speed $\dot{\psi}$. This assumption which, under quasistationary conditions, represents a good approximation, does not strictly hold, for example, for the tracking of objects moving with variable or high speeds. The tracking of objects moving with constant and not too high speed can be treated under quasistationary conditions, as discussed before; see also Virsik and Reichardt (1974). As a matter of fact the quasi-stationary approach is limited to those experimental conditions where the dynamics of the ψ -dependent evaluation mechanism can be neglected. A complete treatment of the general case requires the consideration of a multi-input system with spatially non-homogeneous dynamic properties, developed more recently, Poggio and Reichardt (1973b), Poggio (1974).

As has been mentioned in the discussion of our first paper, Poggio and Reichardt (1973a), Eqs. (1) and (3A) can be extended to describe simple tracking situations. Agreement between theory and experiments has been reported here for the tracking of one object moving at constant speed. The essential validity of our phenomenological equation to describe tracking tasks under natural conditions has been verified in observations of chases between free flying flies; Land and Collett (1974).

In the preceding paper we have considered the transformation which maps the pattern dependent $D(\psi)$ distribution into the orientation distribution $p(\psi)$, under the assumption of a "white" gaussian torque fluctuation process. The effects on this transformation, due to the actual coloured spectral composition of the fluctuation process, have been treated in this paper. In the "white" noise case, the stationary probability distribution is a function of the potential distribution $U(\psi)$ only, whereas in the "coloured" case it is a function of $U(\psi)$ and its first and second derivatives, at least in the range of validity of the approximation derived in Appendix II. As an important consequence of this dependence, a symmetry breaking in the maxima of the stationary orientation behaviour may occur without a corresponding symmetry breaking in the potential minima. This observation shows that quantitative changes in the spectral composition of the fluctuation process can lead to qualitative changes in the stationary behaviour of the system. However, it should be pointed out that in the majority of the situations the white noise hypothesis is completely satisfactory.

Finally a very interesting hint towards the existence of nonlinear inhibitory interactions in the orientation mechanism is provided by our investigations of the validity of the "superposition principle". As expected, the "attractiveness" of neighbouring stripes cannot be the sum of the "attractivenesses" of the individual stripes; according to our data nonlinear inhibitory interactions rather than saturation effects seem to play a major role. From the quantitative failure of the "superposition rule" (for $\Delta\psi < 80^\circ$), it is clear that interactions between input channels affect the "attractiveness" of patterns. Therefore, beside the "direct channels", which probably provide the position information underlying the orientation behaviour towards small objects, Pick (1974), surrounding nonlinear interactions are also present. They might strongly and selectively depend on the spatio-temporal mapping of the specific pattern onto the receptor array; Pick (1974), Geiger and Poggio (1974), Reichardt and Poggio (in preparation). On the other hand for separations larger than 80° the superposition rule seems to represent a satisfactory approximation. If this also holds for more dynamic degrees of freedom, Wehrhahn and Reichardt (1973), a "transitivity law" for spontaneous pattern preference in flies will apply, Poggio (1974), in this range of pattern separations.

A characterization – now in progress – of the functional properties of these interactions is outside the phenomenological level of the present work as it requires a different approach and formalism; Poggio

and Reichardt (1973b), Poggio (1974). We shall report these results later.

The nonlinear interactions underlying the position dependent fly's reaction may provide a powerful mechanism for selective pattern attraction, as suggested by our experiments. They actually might implement a type of distributed parallel processing which seems more powerful than in the case of linear lateral inhibition; Poggio (1974).

A knowledge of the interactive structure should finally lead to the $D(\psi)$ profile and, through the phenomenological theory, to the associated stationary orientation behaviour of the fly for arbitrary patterns.

Appendix I

Since each receptor in the eye of the fly transduces the time course of a local light intensity, evaluation of visual stimuli is obtained from 1 or more interacting inputs. In this sense the actual parameters which determine the "open loop" fly's reaction are the light fluxes onto each receptor rather than the phenomenological quantities ψ and $\dot{\psi}$. A description in terms of interactions can be given by a Volterra series. The light flux into a receptor i is given by

$$x_i(t) = \int \varrho_i(\xi) f[\xi - \psi(t)] d\xi, \quad (I-1)$$

where ϱ_i represents the contrast transfer function of receptor i and f the pattern. For small displacements of a narrow stripe around a given angular position ψ_0 , Eq. (I-1) can be linearized as

$$x_i(t) \approx a_i + b_i \Delta\psi(t), \quad (I-2)$$

which, substituted into the Volterra functional series for the inputs located in the neighbourhoods of ψ_0 , leads to a series in $\psi(t)$, valid for small displacements around ψ_0 . Taking into account that the fly's average reaction is zero if $\dot{\psi} = 0$, we may write, up to quadratic terms,

$$F_{\psi_0}\{\psi(t)\} = \int k_{\psi_0}^{(1)}(t - \tau_1) \Delta\dot{\psi}(\tau_1) d\tau_1 + \iint k_{\psi_0}^{(2)}(t - \tau_1, t - \tau_2) \Delta\dot{\psi}(\tau_1) \Delta\dot{\psi}(\tau_2) d\tau_1 d\tau_2, \quad (I-3)$$

which is valid for movements of small amplitudes around ψ_0 . The nonlinear transformation Eq. (I-3) can be linearized, Poggio and Reichardt (1973), Kasakov (1961) through the statistical linearization method which gives the best (in the least square sense) linear *inertialless* approximation of Eq. (I-3) as

$$F(t) \approx r\dot{\psi}(t) + D(\psi_0), \quad (I-4)$$

with

$$r = \frac{\overline{F\dot{\psi}}}{\overline{\dot{\psi}^2}}, \quad D(\psi_0) = \overline{F},$$

again valid around ψ_0 and dependent on the $\dot{\psi}$ statistics; see Appendix A in Poggio and Reichardt (1973a).

The extension of Eq. (I-4) to describe reactions for movements not restricted to a neighbourhood of ψ_0 is somewhat ill defined. However, the average reaction \overline{F} is known to be rather independent from the frequency of small oscillations, Fig. 5b, in Reichardt (1973), and the inertialless assumption seems reasonable under normal fixation conditions, suggesting the validity of Eq. (I-4) for all ψ . Actually the "quasi-stationary" approximation Eq. (3B) gives

selfconsistently, through Eq. (1), the correct average quantities — like the ψ -probability distribution — which characterize the fixation process.

Whenever the dynamics plays an important role — as in some tracking conditions, where the “memory” of the system and the “history” of the stimulus are highly critical — Eq. (1-4) cannot be considered sufficient any more and a general description must be derived directly in terms of receptor interactions; Reichardt and Poggio (in preparation), Poggio (1974).

Appendix II

In the following we will give the approximated stationary solution, based on a method developed by Stratonovitch (1967), of equation [Eq. (C.3) in Poggio and Reichardt (1973a)]

$$(k+r)\dot{\psi} + \frac{\partial}{\partial \psi} U(\psi) = N(t), \quad (\text{II-1})$$

where $N(t)$ is a coloured gaussian process with the power spectrum $\bar{N}(\omega) = \frac{2A\gamma}{\gamma^2 + \omega^2}$.

A new method will also be developed to give the probability of barrier crossing in this non-white case, generalizing known results of Kramers (1940) concerning the white noise case. These results may also be of interest in connection with the stochastic treatment of generalized tracking systems; see Lindsey (1972).

Although the analytic approximate solutions which we will obtain are not accurate for our parameter values (the probability distributions plotted in Fig. 2a were obtained through digital simulation), nevertheless they fully illustrate the critical role played by the coloured spectrum. Depending on the spectrum of the fluctuations an “early symmetry breaking” in the peaks of the probability distribution can take place *without* a corresponding symmetry breaking in the shape of the potential $U(\psi)$. The effect is a simple illustration of the importance of the *nature* of fluctuations, when not thermal-like (delta-correlated), in determining the phase transition behaviour of a system, see Nicolis and Prigogine (1971). It is easy to check that Eq. (II-1) and the corresponding Fokker-Planck Eq. (II-5) do not satisfy the conditions of detailed balance; Graham and Haken (1971). Therefore no general method is available to obtain the stationary distribution for Eq. (I-1). Equation (II-1) can be rewritten in the phase space [see Eq. (C.6) in Poggio and Reichardt (1973a)] as

$$\dot{\psi} - D(\psi) \frac{1}{k+r} = x(t) \quad (\text{II-2})$$

$$\dot{x} + \gamma x = W' \quad \text{with} \quad S_{W'W'}(\tau) = \frac{2A\gamma}{(k+r)^2} \delta(\tau).$$

Differentiating the first equation, inserting the second and using the first again gives

$$m^2 \ddot{\psi} + \left(1 - m^2 \frac{dH}{d\psi}(\psi)\right) \dot{\psi} - H(\psi) = W''(t) \quad (\text{II-3})$$

where

$$m^2 = \frac{1}{\gamma}$$

$$\frac{D(\psi)}{k+r} = H(\psi)$$

$$S_{W''W''}(\tau) = \frac{2A}{(k+r)^2 \gamma} \delta(\tau).$$

Equation (II-3) can also be rewritten as

$$m\dot{\psi} = v \quad (\text{II-4})$$

$$m\dot{v} + [1 - m^2 H'(\psi)] \frac{v}{m} - H(\psi) = W''$$

and the corresponding Fokker-Planck equation is

$$\frac{\partial p}{\partial t} = - \frac{\partial}{\partial \psi} \left(\frac{v}{m} p \right) - \frac{\partial}{\partial v} \left\{ v H'(\psi) - \frac{v}{m^2} + \frac{H(\psi)}{m} \right\} p + \frac{s}{2m^2} \frac{\partial^2}{\partial v^2} p \quad \text{with} \quad \frac{s}{2} = \frac{A}{(k+r)^2} m^2. \quad (\text{II-5})$$

To find an approximate stationary solution we write the probability density in the form

$$p(\psi, v) = \sum_n p_n(\psi) W_n(v) \quad (\text{II-6})$$

where

$$W_n(v) = \sqrt{\frac{2}{s}} \frac{1}{\sqrt{n!}} F^{(n+1)} \left(\sqrt{\frac{2}{s}} v \right) \\ F^{(n+1)}(z) = \frac{1}{\sqrt{2\pi}} \frac{d^n}{dz^n} e^{-\frac{z^2}{2}}.$$

Since we are interested in the stationary distribution $p(\psi)$, integrating Eq. (II-6) with respect to v gives

$$p(\psi) = \int dv p(\psi, v) = p_0(\psi), \quad (\text{II-7})$$

because

$$\int_{-\infty}^{+\infty} W_n(v) dv = \delta_{n,0}.$$

Therefore we will derive in the following an approximate equation in p_0 . Substituting (II-6) into (II-5), using relations among the W_n , collecting the W_n with the same n and keeping the first three terms of the expansion, Eq. (II-6) gives three equations in $p_0(\psi)$, $p_1(\psi)$, and $p_2(\psi)$. From the three equations we can derive an approximate equation in p_0 which reads

$$\frac{\partial}{\partial t} \left[1 + m^2 \frac{\partial}{\partial \psi} \left(-H + \frac{s}{2} \frac{\partial}{\partial \psi} \right) \right] p_0 = \frac{\partial}{\partial \psi} \left(1 - m^2 \frac{\partial}{\partial t} + m^2 H' \right) \\ \cdot \left(-H + \frac{s}{2} \frac{\partial}{\partial \psi} \right) p_0 \\ + m^2 \frac{\partial^2}{\partial \psi^2} \frac{s}{2} (H' p_0) \\ + \frac{\partial^2}{\partial \psi^2} m^2 \left(-H + \frac{s}{2} \frac{\partial}{\partial \psi} \right)^2 p_0 \\ + O(m^4) \quad (\text{II-8})$$

where $O(m^4)$ indicates terms of order m^4 or higher.

Dividing the two sides by $\left[1 + m^2 \frac{\partial}{\partial \psi} \left(-H + \frac{s}{2} \frac{\partial}{\partial \psi} \right) \right]$ and using the identity

$$\frac{\partial^2}{\partial \psi^2} \left(-H + \frac{s}{2} \frac{\partial}{\partial \psi} \right)^2 - \left[\frac{\partial}{\partial \psi} \left(-H + \frac{s}{2} \frac{\partial}{\partial \psi} \right) \right]^2 \\ = - \frac{\partial}{\partial \psi} \left(\frac{\partial}{\partial \psi} H - H \frac{\partial}{\partial \psi} \right) \left(-H + \frac{s}{2} \frac{\partial}{\partial \psi} \right) \quad (\text{II-9})$$

we obtain

$$\begin{aligned} \frac{\partial}{\partial t} p_0 = \frac{\partial}{\partial \psi} \left\{ \left(1 - m^2 \left(\frac{\partial}{\partial \psi} H - H \frac{\partial}{\partial \psi} \right) + m^2 H' \right) \right. \\ \left. \cdot \left(-H p_0 + \frac{s}{2} \frac{\partial}{\partial \psi} p_0 \right) \right\} \\ + m^2 \frac{s}{2} \frac{\partial^2}{\partial \psi^2} H' p_0 + O(m^4). \end{aligned} \quad (\text{II-10})$$

The stationary solution of Eq. (II-10) — for $\frac{\partial}{\partial t} p_0 = 0$ — represents, according to Eq. (II-7), the approximate stationary solution of Eq. (II-5).

A formal integration with respect to ψ gives

$$\begin{aligned} \text{const} = \left(-H + m^2 \frac{s}{2} H'' \right) p(\psi) \\ + \left(\frac{s}{2} + m^2 \frac{s}{2} H' \right) p(\psi) + O(m^4) \end{aligned} \quad (\text{II-11})$$

which has the solution, at the accuracy chosen before,

$$p(\psi) = \text{const} e^{\frac{2}{s} \int H(\psi) d\psi - \frac{m^2}{s} H^2(\psi) - m^2 \frac{d}{d\psi} H(\psi)}, \quad (\text{II-12})$$

as it can be checked.

Rewriting Eq. (II-12) as

$$p(\psi) = \text{const} e^{-\frac{\gamma}{A}(k+r)U(\psi) - \frac{1}{2A}D^2(\psi) - \frac{1}{\gamma(k+r)}\frac{dD(\psi)}{d\psi}}, \quad (\text{II-13})$$

it becomes obvious that $p(\psi)$ may present two maxima even if $U(\psi)$ has only one minimum (early phase transition). For instance a flat potential with sharp rising edges will have this property. The strength of this effect depends critically on the spectral composition of the fluctuations.

It is also possible, using Eq. (II-13), to find an alternative solution to the problem of barrier crossing (with non-white noise) already outlined in Appendix C of Poggio and Reichardt (1973a).

Equation (C.21) in Poggio and Reichardt (1973a) through the substitution $x(t) = w - \frac{D(\psi)}{k+r}$ gives for $\psi' = 0$,

$$p(\psi' = 0, w) = C'' e^{-\frac{A}{2d}w^2} \sqrt{\frac{\Gamma}{2\pi d}} \int_{-\infty}^w d\zeta e^{-\frac{\Gamma}{2d}\zeta^2}. \quad (\text{II-14})$$

Because of our quasi stationary conditions Eq. (C.17) and Eq. (C.21) must become identical in the limit $\zeta \rightarrow \infty$, giving

$$C'' = C'. \quad (\text{II-15})$$

Equation (II-13) around ψ_b and Eq. (C.20) allow us to find the value C' as

$$C' = \text{const} \sqrt{\frac{\Delta}{2\pi d}} e^{-\frac{\Gamma}{\gamma}} e^{-\frac{\gamma}{A}(k+r)E}. \quad (\text{II-16})$$

Equation (II-13) around ψ_0 gives the normalization factor

$$\text{const} = \sqrt{\frac{l\gamma(l+\gamma)}{2\pi d}} e^{-\frac{1}{\gamma}}. \quad (\text{II-17})$$

Equations (II-17), (II-16), (II-15) serve to normalize C'' of Eq. (II-14) which can be used now to provide the probability flow across the barrier

$$j_b = \int_{-\infty}^{+\infty} p(\psi' = 0, w) w dw. \quad (\text{II-18})$$

An integration by parts gives

$$j_b = C'' \sqrt{\frac{\Gamma}{\Delta + \Gamma}} \frac{d}{d}, \quad (\text{II-19})$$

which can be rewritten, as probability of barrier crossing, normalizing C'' through Eqs. (II-17), (II-16), (II-15),

$$p_b = \frac{1}{2\pi} \frac{1}{k+r} \sqrt{\frac{\gamma + \frac{\alpha}{k+r}}{\alpha'}} \sqrt{\alpha\alpha'} e^{-\frac{\alpha+\alpha'}{\gamma(k+r)}} e^{-\frac{\gamma}{A}(k+r)E}. \quad (\text{II-20})$$

which is valid under quasi stationary assumptions and in the same approximation of Eq. (II-13) (γ great enough). Clearly in the white noise case ($\gamma \rightarrow \infty$, $A = c\gamma$) Eq. (II-20) becomes consistently Eq. (4.1). Moreover under the condition $\gamma(k+r) > (\alpha + \alpha')$ Eq. (II-20) is well approximated by Eq. (C.27), whose range of validity is more restricted.

A number of alternative approaches to the type of problems treated in this as well as in the next Appendix are available and will be discussed elsewhere.

Appendix III

In the case of a stripe moving at constant speed the tracking equation, derived from Eqs. (1) and (3A), is

$$(r+k)\dot{\psi} + \frac{\partial}{\partial \psi} \{U(\psi)\} = N(t) + V, \quad (\text{III-1})$$

where V represents the voltage (in dyn cm) added into the closed loop system in order to simulate an object moving at constant angular velocity $w = \frac{V}{k}$. In Eq. (III-1) the parameter θ is assumed

to be equal to zero (as in Appendix II) because of its very small value. The coordinate ψ represents the angular error between the fly's direction of flight and the position of the object. The noise $N(t)$ is assumed to be gaussian white, with an autocorrelation $S_{NN}(\tau) = 2c\delta(\tau)$.

The statistics of the process $\psi(t)$ can be given exactly by the Fokker-Planck technique, which associates with Eq. (III-1) — interpreted in the usual way as an Ito equation — the following partial differential equation in the probability density $p(\psi, t)$

$$\frac{\partial p}{\partial t} = -\frac{\partial}{\partial \psi} \left(\frac{D^*(\psi)}{k+r} p \right) + \frac{c}{(k+r)^2} \frac{\partial^2 p}{\partial \psi^2}, \quad (\text{III-2})$$

with $D^*(\psi) = V - \frac{\partial U(\psi)}{\partial \psi}$.

The stationary solution $p(\psi)$ must satisfy to

$$\frac{d^2 p}{d\psi^2} - \frac{d}{d\psi} \left(\frac{k+r}{c} D^*(\psi) p \right) = 0, \quad (\text{III-3})$$

to the boundary condition

$$p(\pi) = p(-\pi), \quad (\text{III-4})$$

and to

$$\int_0^{2\pi} p(\psi) d\psi = 1. \quad (\text{III-5})$$

Integrating once, Eq. (III-3) gives

$$\frac{dp}{d\psi} = C_1 + \frac{(k+r)}{c} D^*(\psi) p(\psi). \quad (\text{III-6})$$

The general integral of Eq. (III-6) is given by the integrant factor method as

$$p(\psi) = C_1 e^{\int d\psi \frac{k+r}{c} D^*(\psi)} \int_{C_2} e^{-\int \frac{k+r}{c} D^*(\psi) d\psi} d\psi. \quad (\text{III-7})$$

In order to satisfy Eq. (III-4) C_2 is chosen as

$$C_2 = \psi - 2\pi. \quad (\text{III-8})$$

Defining $U^*(\psi) = V\psi - U(\psi)$, Eq. (III-7) can be rewritten as

$$p(\psi) = C_1 e^{\frac{k+r}{c} U^*(\psi)} \int_{\psi-2\pi}^{\psi} e^{-\frac{k+r}{c} U^*(\psi')} d\psi', \quad (\text{III-9})$$

with C_1 given by the normalization condition, Eq. (III-5). When $V \equiv 0$ the equation reduces consistently to Eq. (31) of Poggio and Reichardt (1973a).

The probability distribution Eq. (III-8) can be interpreted as the probability distribution of a brownian particle in an external field of forces generated by the (non cyclic) potential $U^*(\psi) = V\psi - U(\psi)$. The behaviour of the fly in this tracking situation, as modelled by Eq. (III-1), if formally equivalent to that of a coherent tracking loop, which is a communication receiver operating as a coherent detector. Other results, related to Eq. (III-9), can be found in the literature on the subject; see Stratonovitch (1967), Lindsey (1972). This analogy with a class of modern tracking systems can be useful in discussing in which sense the fly's tracking behaviour is optimal; it may even embed a much deeper meaning, pointing towards general mechanisms which may underly the orientation behaviour in insects; Poggio (in preparation).

Acknowledgements. We thank L. Heimbürger for his valuable technical assistance and for drawing the figures of this paper. E. Buchner, G. Geiger, Professor K. G. Götz, Dr. M. Heisenberg, B. Pick, Dr. R. Virsik, and Dr. Ch. Wehrhahn have contributed with important comments. We would like to thank Mrs. E. Ockelford for correcting and Mrs. I. Geiss for typing the English manuscript.

References

Geiger, G.: Optomotor responses of the fly *Musca domestica* to transient stimuli of edges and stripes. *Kybernetik* **16**, 37—43 (1974)

- Geiger, G., Poggio, T.: The orientation of flies towards visual patterns: on the search for the underlying functional interactions. *Biol. Cybernetics* **19** (1975) (in press)
- Graham, B., Haken, H.: Generalized thermodynamic potential for Markoff systems in detailed balance. *Z. Physik* **243**, 289 (1971)
- Kasakov, I. E.: Automatic and remote control. Proc. I. Int. Congr. IFAC, Moscow 1960. Ed. Coales J. F. London: Butterworth 1961
- Kramers, H. A.: Brownian motion in a field of force. *Physica* **VI**, 4, 284 (1940)
- Land, M. F., Collett, T. S.: Chasing behaviour of houseflies (*Fannia canicularis*). *Z. comp. Phys.* **89**, 331 (1974)
- Lindsey, W. C.: Synchronization systems in communication and control. Hemel-Hempstead: N. J. Prentice-Hall, Inc. 1972
- Nicolis, G., Prigogine, I.: Fluctuations in nonequilibrium systems. *Proc. nat. Acad. Sci. (Wash.)* **68**, 9, 2102 (1971)
- Pick, B.: Visual flicker induces orientation behaviour in the fly *Musca*. *Naturforsch.* **29c**, 310 (1974)
- Poggio, T.: Processing of visual information in flies: from a phenomenological model towards the nervous mechanisms. Proc. of the I Symp. of the It. Soc. Biophysics, ed. A. Vecchi Tipo Lito Parma 1974
- Poggio, T., Reichardt, W.: A theory of the pattern induced flight orientation of the fly *Musca domestica*. *Kybernetik* **12**, 185 (1973a)
- Poggio, R., Reichardt, W.: Considerations on models of movement detection. *Kybernetik* **13**, 223 (1973b)
- Reichardt, W.: Musterinduzierte Flugorientierung der Fliege *Musca domestica*. *Naturwissenschaften* **60**, 122 (1973)
- Stratonovitch, R. L.: Topics in the theory of random noise I, II. New York: Gordon and Breach 1967
- Virsik, R., Reichardt, W.: Tracking of moving objects by the fly *Musca domestica*. *Naturwissenschaften* **61**, 132 (1974)
- Wehrhahn, C., Reichardt, W.: Visual orientation of the fly *Musca domestica* towards a horizontal stripe. *Naturwissenschaften* **60**, 203 (1973)

Prof. W. Reichardt
Dr. T. Poggio
Max-Planck-Institut
für biologische Kybernetik
D-7400 Tübingen,
Spemannstraße 38
Federal Republic of Germany